JOURNAL OF MATERIALS SCIENCE 31 (1996) 5817–5820

Translucent low-thermal expansion ceramics

BIAO ZHANG, JINGKUN GUO, HANMEI YANG
Shanghai Institute of Ceramics, Chinese Academy of Sciences, Shanghai 200050, Peoples Republic of China

PEINAN ZHU
Department of Materials Science and Engineering, Tongji University, Shanghai 200092, Peoples Republic of China

The optical transmittance of pressureless sintered $KZr_2P_3O_{12}$ (KZP) ceramics was studied in the ultraviolet, visible light, and near infrared spectrum ranges. Thermal expansion, strength, and thermal shock resistance of the ceramics were also studied. KZP ceramics with different additives (0–8 wt% of MgO, ZnO or SrO) show a 30–70% transmittance from 0.4–2 μm, a low thermal expansion coefficient and high thermal shock resistance. These polyfunctional ceramics might be useful as optical windows.

1. Introduction

The $NaZr_2P_3O_{12}$ (NZP) family of ceramics are low thermal expansion materials and have attracted serious attention due to a variety of useful properties [1–4]. The crystal structure of the potassium analogue KZP permits ionic substitutions at various lattice sites in the structure and the formation of solid solutions [5]. The crystallinity of KZP can be improved by the sol–gel process [6]. The linear thermal expansion coefficient of KZP ceramics is nearly zero [7]. The critical grain size for microcracking of KZP is 5.5 μm [8].

Optically transparent ceramics, such as Al_2O_3 and Y_2O_3, are widely used in the lighting industry due to their excellent thermal shock resistance and high temperature strength. Recent interest in optically translucent ceramics, such as mullite and spinel [9, 10], has focused on their applicability as a window material at elevated temperature in the mid-infrared range. In the present work, the optical properties, thermal expansion, strength and thermal shock resistance of pressureless sintered ceramics have been investigated.

2. Experimental procedure

$KZr_2P_3O_{12}$ (with 0–8 wt % MgO, ZnO, or SrO) powder was synthesized by mixing stoichiometric amounts of the precursor solutions of $NH_4H_2PO_4$ and $ZrOCl_2 \cdot 8H_2O$. The precipitate was filtered to remove Cl^- ions and then the precipitate was remixed with KNO_3 solution, dried at 120 °C and calcined between 700–1000 °C. The detailed process for the preparation of powders was described in an earlier publication [11].

The powder sample was moulded into a plate (40 mm dia. × 5 mm). The samples were pressed to 50 MPa by a uniaxial press and then at 100 MPa by a hydrostatic press. Green samples were preheated at 500 °C in air to eliminate any organic binder and then heated to 1150–1250 °C for 0.5–5 h in air.

The thermal expansion was measured using a dilatometer (Model 402ES-3, Netzsch) on a $4 \times 4 \times 50$ mm^3 sintered sample from 25–1000 °C at a heating rate of 10 °C per min. The bulk density of the sintered ceramics was determined by the Archimedes method. The flexural strengths were measured by the three point bending test on bar specimens ($2.5 \times 5 \times 35$ mm^3) over a 20 mm span at a cross head speed of 0.5 mm per min (Instron model 1195) before and after a thermal shock in water (0 °C).

Optical transmittance measurements were performed on 30 mm dia. × 0.5 mm specimens using a Cary-2390 UV-VIS-NIR spectrophotometer with an integration globe from 0.2–2.2 μm. The microstructures of the samples were examined by scanning electron microscopy (SEM: model EPMA-8705Q_{II}) and transmission electron microscopy (TEM: model JEM-200CX) and high resolution electron microscopy (HREM). The total stresses of specimens before and after the thermal shock were measured by X-ray diffraction (XRD) method at fixed Ψ (model D/Max-3A). The total residual stress (σ, include macrostresses and microstresses) is approximated by the following equation:

$$\sigma = E \cot\Theta \cdot \Delta 2\Theta \cdot \pi/(2(1 + \nu)\Delta \sin\Psi 180) \quad (1)$$

where Ψ is the angle between the sample surface and diffraction crystal face, Θ is the diffraction angle, $\Delta 2\Theta$ is the difference with diffraction angle when $\Psi = 0°$ and $\Psi = 45°$. E and ν are the Young's modulus and Poisson's ratio respectively.

3. Results and discussion

3.1. Sintering and thermal expansion

The theoretical density of pure $KZr_2P_3O_{12}$ is 3.22 g cm^{-3}. The sintered densities of specimens fired at different temperatures and times are shown in

0022–2461 © *1996 Chapman & Hall*

Fig. 1. The maximum density achieved was about 99.3% of theoretical with a sintering temperature of 1200 °C and a holding time of 1 h. However there were still some pores as is illustrated in Fig. 2. An SEM study of the fractured surface reveals that the porosities are located in the grain boundary and that in general the grain size is quite uniform. These pores can be easily removed by HP (hot pressing) or HIP (hot isostatic pressing) process.

The thermal expansion coefficients of the ceramic were calculated in the temperature range of 25–1000 °C and are presented in Table I. As is evident from these results, the ceramic exhibits an almost zero expansion. Examples of selected properties, such as density, strength, fracture toughness, Young's modulus, Poisson's ratio and thermal conductivity, are summarized in Table II.

The thermal expansion of NZP based materials is greatly influenced by interstitial ions. An ion with a larger ionic radius (K^+) results in a lower thermal expansion. KZP has a high thermal expansion anisotropy and a negative thermal expansion [8]. The addition of a small amount of MgO, ZnO or SrO markedly increases the thermal expansion.

3.2. Thermal shock resistance

The thermal shock resistance was evaluated by measuring the residual flexural strength of specimens water quenched from various temperatures. Fig. 3a shows the flexural strength of specimens after the water quench. With an increase in the quench temperature, the retained strength increases gradually from 300–800 °C. When quenched above 800 °C, the strength of the specimens decreases slowly as opposed to a sudden change. After quenching at 1000 °C the strength is the same as that of an as sintered sample.

For a more detailed study of the phenomenon, the surface residual stress was determined by the X-ray diffraction method described in Equation 1. The results are shown in Fig. 3b, the negative value denotes a compressive stress. The more negative the value, the larger the strength. The surface stress formed by quenching at 600 °C is almost two times that of an unquenched sample. In neither the optical microscopy nor the scanning electron microscopy, could obvious cracks be observed. This is evidence that the ceramic has excellent thermal shock resistance. The ΔT_c, the maximum step change in temperature that can be sustained without fracture, is higher than 800 °C.

The reason that the strength increases with an increasing quench temperature is that the ceramic has a low thermal expansion. Below 300 °C the ceramic exhibits a negative expansion, above 300 °C, it is positive. When quenched, the outer surface of the specimen cools quickly and shrinks until 300 °C, and then expands below 300 °C. However the core of the sample cools slowly and is still shrinking while the outer surface is already below 300 °C. Thus, the outer surface is constrained and compressive stresses are formed on the surface, the strength is raised in a similar manner to that of strengthened glass. Another reason

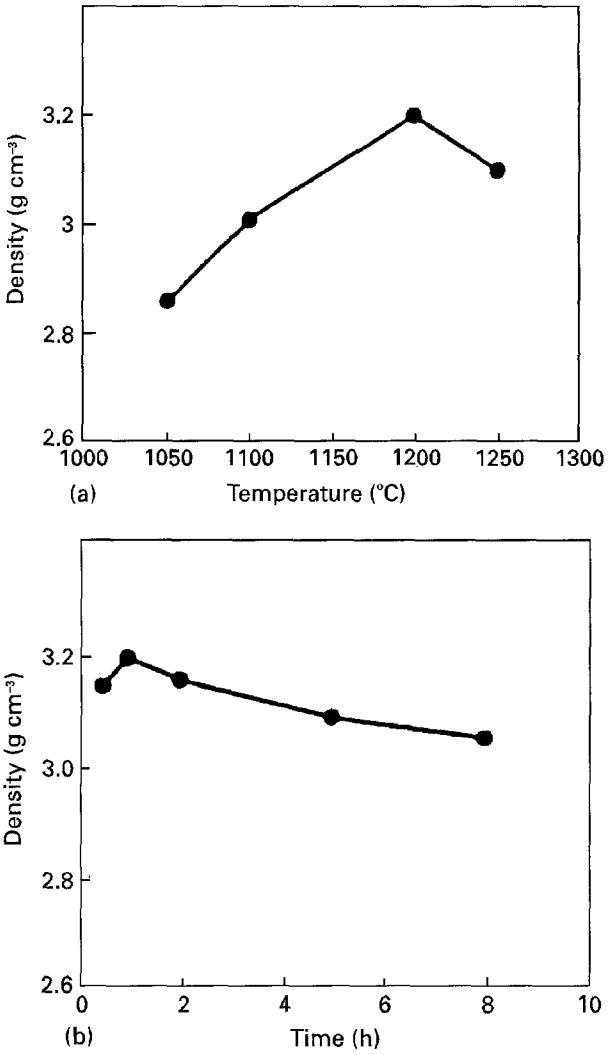

Figure 1 Variation of density with (a) sintering temperature (2 h), and (b) sintering time (1200 °C).

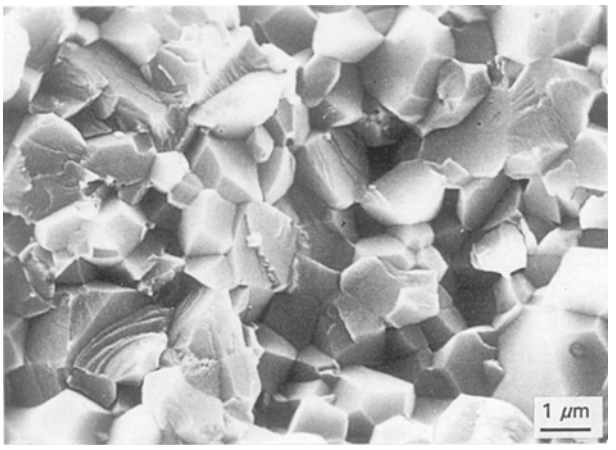

Figure 2 SEM photograph of the microstructure of KZP ceramic.

TABLE I Thermal expansion of a KZP ceramic

T (°C)	100	200	300	400	500	600	700	800	900	1000
$\alpha(\times 10^{-6}$ per °C)	− 1.8	− 1.2	− 0.6	0.4	1.05	1.19	1.25	1.35	1.46	1.52

TABLE II Properties of the KZP ceramic

Density (g cm^{-3})	3.2
Young's modulus (GPa)	109
Poisson's ratio	0.27
Bending strength (MPa)	101
Fracture toughness (MPa $m^{1/2}$)	2.0
Specific heat at 500 °C (J/g · K)	0.92
Thermal conductivity at 500 °C (W/m · K)	1.6

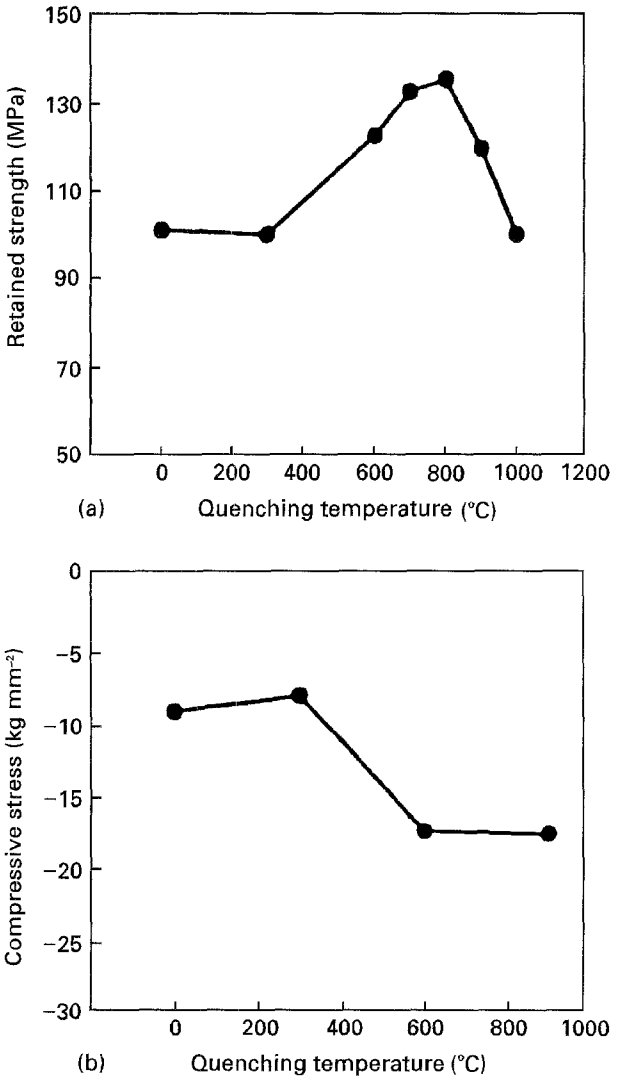

Figure 3 (a) Thermal shock resistance, and (b) compressive stress variation with quenching temperature of the KZP ceramic.

for the high thermal shock resistance of the ceramic may be due to the point that there are no glass phases at intergranular boundaries. It has been suggested by Hoffmann [12] that the ΔT_c may be connected with the softening of a glass phase.

3.3. Optical transmission

The optical transmittance of the ceramic in ultraviolet (UV), visible light (VIS) to near infrared (NIR) ranges is shown in Fig. 4. The transmittance of the ceramic is very low in the UV region, but becomes significantly higher in VIS (~ 40%) and NIR (~ 70%).

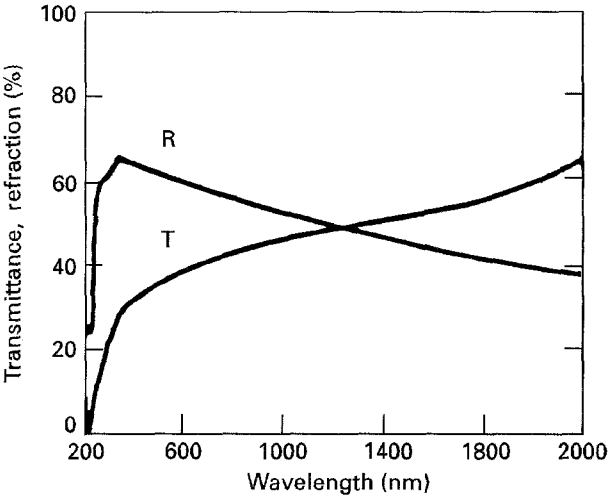

Figure 4 Spectral transmittance (T) and refraction (R) of the KZP ceramic in the UV-VIS-NIR range.

In general, in the preparation of a transparent polycrystalline material, a number of critical requirements have to be met, of which the most important are (1) high chemical purity, (2) low porosity, (3) phase purity or a minimal difference in the refractive index between the adjacent phases, (4) absence of microcracks, and (5) the size of the scattering centres should not be in the Rayleigh and Mie scattering range and the grain size should be less than the wavelength of the transmitted radiation for a non-cubic crystal. It is easily to satisfy conditions (2) and (5) by choosing a suitable preparation process (such as HIP). For the KZP ceramic, microcracks caused by anisotropic expansion which are its major disadvantage can be improved by molecular scale compositional designing [3]. Phase purity is the most significant advantage of KZP ceramics since with its "open structure" and a relatively rigid framework. It permits an enormous range of ionic substitution with no effect on the crystallography of the structure. The substitutions can be complete or partial, leading to a remarkable richness of solid solution behaviour. Fig. 5a shows a TEM micrograph of the ceramic. It is clear that there are no integranular phases or impurities at triple grain junctions or the two grain boundaries. In Fig. 4, the low transmittance and refraction in the UV regime may be caused by charge transfer absorption and/or Mie scattering. Scattering caused by submicrometre inhomogeneities and refraction which takes place on the surface and also at phase boundaries as well as on grain boundaries of the non-cubic crystal are factors which influence the translucency. The birefringence leading to a change of refraction index at randomly orientated grain boundaries causes the refraction. For a KZP ceramic, an improvement of grain boundary refraction and pore scattering will produce a high transmittance. The HREM image presented in Fig. 5b shows the lattice fringes of two grains that meet each other at the boundary and the electron diffraction pattern in a polycrystalline area. Light translucency of a 0.5 mm thick dense KZP ceramic is shown in Fig. 6. The optical properties of KZP ceramics prepared by HIP are currently under investigation.

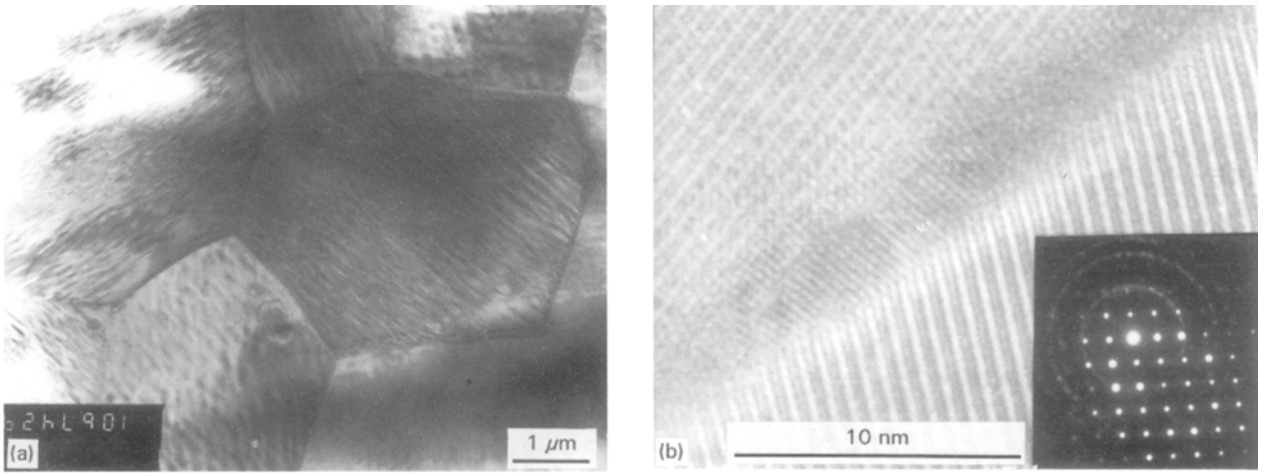

Figure 5 (a) TEM micrograph and (b) HREM image of the KZP ceramic.

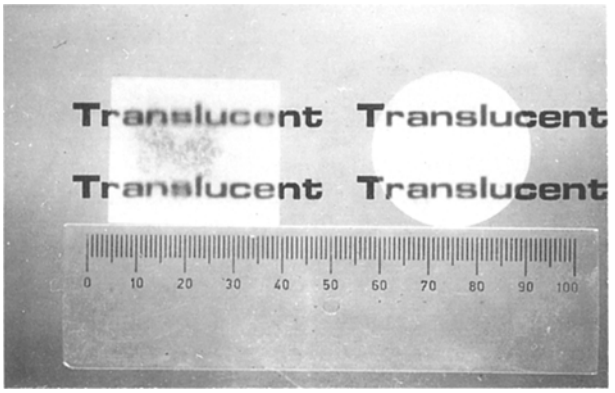

Figure 6 Optical translucency of the KZP ceramic.

The main application of transparent ceramics is as windows in chemically harsh, hot, or mechanically stressful environments [13]. The KZP ceramic studied here is a potential high temperature optical window material due to its low thermal expansion, high thermal shock resistance, translucent behaviour, low sintering temperature, and low cost.

4. Summary

A multifunctional ceramic $KZr_2P_3O_{12}$ containing 0–8 wt % additives has been investigated. The ceramic with a 99.3% theoretical density exhibits a low thermal expansion (1.52×10^{-6} per °C, between 25–1000 °C), a high thermal shock resistance (> 800 °C) and optical translucency (30–70% transmittance in the VIS–NIR range). The ceramic may be expected to find use as an optical window in high temperature applications.

References

1. R. ROY, D. K. AGRAWAL and H. A. MCKINSTRY, *Ann. Rev. Mater. Sci.* **19** (1989) 59.
2. S. Y. LIMAYE, D. K. AGRAWAL and H. A. MCKINSTRY, *J. Amer. Ceram. Soc.* **70** (1987) C232.
3. B. ZHANG, J. K. GUO and P. N. ZHU, *Ceram. Int.* **20** (1994) 287.
4. T. OTA and I. YAMAI, *J. Amer. Ceram. Soc.* **69** (1986) 1.
5. M. SLJUKIC, B. MATKOVIC and B. PRODIC, *Z. Krist.* **130** (1969) 148.
6. G. E. LENAIN, H. A. MCKINSTRY and D. K. AGRAWAL, *J. Amer. Ceram. Soc.* **68** (1985) C224.
7. T. OTA and I. YAMAI, *J. Ceram. Soc. Jpn.* **95** (1987) 531.
8. I. YAMAI and T. OTA, *J. Amer. Ceram. Soc.* **76** (1993) 487.
9. I. A. AKSAY, D. M. DABBS and M. SARIKAYA, *ibid.* **74** (1991) 2343.
10. H. SCHNRIDER, M. SCHMUCKER, K. IKEDA and W. A. KAYSSER, *ibid.* **76** (1993) 2912.
11. B. ZHANG, J. K. GUO and P. N. ZHU, *J. Chinese Ceram. Soc.* **22** (1994) 246.
12. R. RAJ, *J. Amer. Ceram. Soc.* **76** (1993) 2147.
13. S. PROCHZAKA and F. J. KLUY, *ibid.* **66** (1983) 874.

Received 1 June 1994
and accepted 13 February 1996